CRYSTAL GROWTH & DESIGN

Article

Tuning of the critical temperature in magnetic 2D coordination polymers by mixed crystal formation

Carsten Wellm, Micha# Rams, Tristan Neumann, Magdalena Ceglarska, and Christian Näther

Cryst. Growth Des., **Just Accepted Manuscript** • DOI: 10.1021/acs.cgd.8b00245 • Publication Date (Web): 26 Mar 2018

ACS Publications

Crystal Growth & Design is published by the American Chemical Society. 1155 Sixteenth Street N.W., Washington, DC 20036

Tuning of the critical temperature in magnetic 2D coordination polymers by mixed crystal formation

Carsten Wellm,[†] *Michał Rams,*[‡] *Tristan Neumann,*[†] *Magdalena Ceglarska,*[‡] *and Christian Näther**[†]

[†]Institut für Anorganische Chemie, Christian-Albrechts-Universität zu Kiel, Max-Eyth-Straße 2, 24118 Kiel, Germany.

[‡]Institute of Physics, Jagiellonian University, Łojasiewicza 11, 30-348 Kraków, Poland.

Abstract: Reaction of $Co(NCS)_2$ and $Ni(NCS)_2$ with 4-acetylpyridine under different conditions leads to the formation of mixed crystals of the layered compound with the composition $[Co_xNi_{1-x}(NCS)_2(4\text{-acetylpyridine})_2]_n$ (x = 0.15 0.3, 0.5 and 0.7). Mixed crystal formation was investigated by a combination of X-ray powder diffraction (XRPD), atomic absorption spectroscopy (AAS), simultaneously scanning electron microscopy (SEM) and energy dispersive X-ray spectroscopy (EDX), differential scanning calorimetry (DSC) as well as magnetic and heat-capacity measurements. Dependent on the synthetic method, homo- or heterogenous mixed crystals were obtained as already indicated by XRPD, where significant differences to the pattern of physical mixtures of the homometallic counterparts $[M(NCS)_2(4\text{-acetylpyridine})_2]_n$ with M = Co or Ni) with the same Co:Ni ratio are observed. Mixed crystals can also be obtained from physical mixtures under thermodynamic control, indicating that they are more stable than the homometallic compounds. This is further supported by AAS, which indicates that the solubility of the mixed crystals is lower than that of the homometallic compounds. Magnetic and heat-capacity

measurements show a linear increase of the critical temperature of magnetic ordering with increasing Ni content and also confirm that homogenous samples were obtained.

INTRODUCTION

In recent years, the development of strategies for a rational synthesis of new coordination polymers with defined magnetic properties has attracted much attention.[1-8] In most cases homometallic compounds were prepared with a variety of ligands that can mediate magnetic exchange differently.[1-8] The magnetic properties of coordination compounds can also be modified by the synthesis of bimetallic compounds, which is in most cases more difficult, but can be achieved using ligands, that can coordinate to different metal cations.[9-11] A very effective strategy consists of the reaction of predefined metal containing building blocks that are linked by other metal cations into coordination polymers of different dimensionality.[12-24] Compared to this, only a very few papers report on the synthesis of mixed crystals of paramagnetic metal cations as an additional tool to modify or tune the magnetic properties of coordination compounds in more detail and some selected examples are given in the reference list.[25-29] This is surprising, because this synthetic strategy is used for decades in inorganic solid state chemistry e.g. for optimization of Mn-Zn soft ferrites [30], bandgap tuning in $Al_xGa_{1-x}As$ semiconductors [31], inducing high-temperature superconductivity in $La_{2-x}Sr_xCuO_4$ [32] or colossal magnetoresistance in $La_{1-x}Sr_xMnO_3$.[33]

There are surely many reasons for such a situation. First of all the synthesis of pure samples of coordination compounds is sometimes difficult to achieve, because in solution different compounds might be in equilibria, which can lead to the formation of mixtures of different compounds. The situation is more complicated when different but chemically very similar metal cations are used because also physical mixtures of the homometallic compounds can form. However, if mixed crystals may have been obtained, the question arises, if their metal ratio corresponds to that used in the synthesis, which is not necessarily the case. It is also of importance to investigate if "homogenous" mixed crystals are obtained or if the metal to

metal ratio varies for different crystals. Finally, if metal cations are used that are neighbors in the periodic table, mixed crystal formation is more difficult to prove.

In this context it is noted that we are interested in coordination polymers based on 3d transition metal cations and thio- or selenocyanate anions for several years.[34-39] Even if the magnetic exchange of these ligands is usually weaker than that of, e.g. azides, these pseudohalide anions show a variety of coordination modes and thus, can form structures of different dimensionality.[40-56] With monodentate co-ligands, like simple pyridine derivatives substituted in 4-position chain structures are usually observed, in which the metal cations are linked by pairs of anionic ligands into chains.[57] Dependent on the nature of the co-ligand, linear or zig-zag-like chains can form, in which the metal cations are differently coordinated including a *trans* or a *cis*-*cis*-*trans*-coordination at the metal center.[58] Finally, if other pyridine derivatives are used, also 2D thiocyanate networks can be obtained, in which the metal cations are linked by the anionic ligands into layers.[59-63]

This is observed, e.g., in the crystal structure of compounds with the composition $[M(NCS)_2(4\text{-acetylpyridine})_2]_n$ for M = Co (**1-Co**) or M = Ni (**1-Ni**) as ligand, for which two isomers exists. The thermodynamic stable form at room-temperature consists of $M(NCS)_2$ dimers that are linked by single anionic ligands into layers that are parallel to the *a*/*b*-plane, whereas the metastable isomer forms linear chains (Fig. 1).[62, 63] In the layered compounds dominating ferromagnetic interactions are observed for **1-Co** and **1-Ni** and both of these compound show magnetic ordering at a critical temperature, which is much lower for the Co compared to the Ni compound.[61, 62]

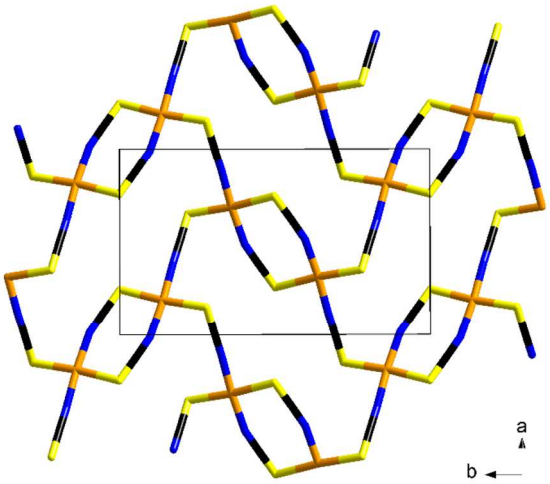

Figure 1. View of the $M(NCS)_2$ coordination network in $[M(NCS)_2(4\text{-acetylpyridine})_2]_n$ (**1-Co** and **1-Ni**). The 4-acetylpyridine ligands are omitted for clarity (M = orange; C = black; N = blue; S = yellow).

Based on these results the question arise whether homogenous mixed crystals with the composition $[Co_xNi_{1-x}(NCS)_2(4\text{-acetylpyridine})_2]_n$ (**1-Co_xNi_{1-x}**) can be prepared, if they still show a phase transition and if this is the case, if the critical temperature can be tuned as a function of the actual Co:Ni ratio. The mixed crystal formation and homogeneity of the samples prepared by different routes was investigated by a combination of atomic absorption spectroscopy (AAS), scanning electron microscopy (SEM) with simultaneous energy dispersive X-ray spectroscopy (EDX), differential scanning calorimetry (DSC), X-ray powder diffraction (XRPD) as well as magnetic and heat-capacity measurements. Both 2D compounds are isotypic and, because both metal cations are neighbored in the periodic table, only very small differences in their XRPD pattern are expected, which is already indicated by their calculated pattern (Table S1 and Figure S1 in the SI). Therefore, the powder pattern of the mixed crystals were always compared with that of physical mixtures of **1-Co** and **1-Ni** with the same Co:Ni ratio.

EXPERIMENTAL SECTION

Reagents. $Co(NCS)_2$, $Ba(NCS)_2{\cdot}3H_2O$ and 4-acetylpyridine were obtained from Alfa Aesar, $Ni(SO_4)_2{\cdot}6H_2O$ was purchased from Merck. All chemicals and solvents were used without further purification. $Ni(NCS)_2$ was prepared by a reaction of equimolar amounts of $NiSO_4{\cdot}6H_2O$ and $Ba(NCS)_2{\cdot}3H_2O$ in water. The resulting precipitate of $BaSO_4$ was filtered off, and the solvent was removed completely using a rotary evaporator leading to a green residue of $Ni(NCS)_2$. The purity was checked by XRPD.

Synthesis of 1-Co. Crystalline powders were obtained by stirring a mixture of $Co(NCS)_2$ (175mg, 1 mmol) and 4-acetylpyridine (222 µL, 2 mmol) in ethanol (1.5 mL) for 2 d. The purity was checked by XRPD and by IR spectroscopy (Figure S2 and S3).[63]

Synthesis of 1-Ni. Crystalline powders were obtained by stirring a mixture of $Ni(NCS)_2$ (175mg, 1 mmol) and 4-acetylpyridine (222 µL, 2 mmol) in ethanol (4 mL) for 2 d. The purity was checked by XRPD and by IR spectroscopy (Figure S4 and S5).[62]

Synthesis of 1-Co_xNi_{1-x}. Crystalline powders were obtained by dissolving $Co(NCS)_2$ and $Ni(NCS)_2$ completely in the desired ratio in ethanol. Afterwards a stoichiometric amount of 4-acetylpyridine was added to the clear solution and the reaction mixture was stirred for 2 d.

Elemental Analysis. CHNS analysis was performed using a EURO EA elemental analyzer, fabricated by EURO VECTOR Instruments and Software.

Scanning electron microscopy (SEM) and energy dispersive X-ray spectroscopy (EDX). These measurements were performed using a Philips ESEM XL 3 with an EDAX New XL-30 Detector, at an acceleration voltage of 20 kV.

Atomic absorptions spectroscopy (AAS). The AAS experiments were performed with a Perkin Elmer Aanalyst 300. Each sample was dissolved in water with 2.5 mL HNO_3 for 100 mL analyte.

IR spectroscopy. The IR data were measured using a Genesis Series FTIR Spectrometer with WINFIRST control software from ATI Mattson.

Differential scanning calorimetry (DSC). The DSC experiments were performed using a DSC 1 star system with STARe Excellence software from Mettler-Toledo AG under dynamic nitrogen atmosphere. The instrument was calibrated using standard reference materials.

Magnetic measurements. All magnetic measurements were performed using a Physical Property Measurement System (PPMS) from Quantum Design, which was equipped with a 9 T magnet, and using QD MPMS-5XL squid magnetometer. The data were corrected for core diamagnetism.

Specific heat measurements. Specific heat was measured by the relaxation technique using a Quantum Design PPMS. Powder samples were pressed into pellets. Apiezon N grease was used to ensure thermal contact of the samples with the calorimeter. The heat capacity of the grease was measured before each run and subtracted.

X-Ray Powder Diffraction (XRPD). The XRPD measurements were performed by using a Stoe Transmission Powder Diffraction System (STADI P) with CuKα radiation that was equipped with a linear position-sensitive MYTHEN detector from STOE & CIE. All measurements were performed with Zn as internal standard.

RESULTS AND DISCUSSION

Synthetic investigations. To investigate if one can differentiate between the homometallic compounds by XRPD, physical mixtures of **1-Co** and **1-Ni** in different Co:Ni ratios with additional Zn as internal standard were measured. As expected, most reflections overlap but the 043 reflections observed at 2-Theta = 25.02° for **1-Co** and at 25.18° for **1-Ni** are successfully resolved (Figure S6). Moreover, the intensity ratio between the 043 reflections for these compounds nicely changes with the Co:Ni ratio and even metal contents of 15% for Co can be proven. We also have investigated these physical mixtures by IR spectroscopy to check

if two bands for the CN stretching vibrations are observed, but they are not successfully resolved and thus, do not allow to prove mixed crystal formation (Figure S7). Finally, these mixtures were also investigated by DSC measurements, and the comparison with the homometallic counterparts shows an additional thermal event that can be traced back to the different decomposition temperatures of the Co and the Ni compound (Figure S8). For mixed crystals only one peak would be expected.

To determine the solubility of both compounds, which might influence the mixed crystal formation, a suspension of **1-Co** and **1-Ni** was stirred in ethanol, from which no solvate can form, filtered off and the metal content was determined by AAS in the filtrate. This shows that the solubility of **1-Co** (6.18 g/L) is significantly higher than that of **1-Ni** (1.15 g/L) (Table S2). Immediate XRPD measurements of the filtered residue prove that no other crystalline phase has formed, which would influence the outcome of this experiment.

In the beginning it was tried to prepare mixed crystals following the procedure for the synthesis of the homometallic compounds, where the metal thiocyanate were added simultaneously to a small amount of solvent.[62, 63] Therefore, a mixture of $Co(NCS)_2$, $Ni(NCS)_2$ and 4-acetylpyridine was stirred in different molar ratios in a small amount of ethanol and the residues that formed within 2 d were investigated by XRPD. It is noted that, e.g., water cannot be used as solvent, because hydrates with the composition $M(NCS)_2(H_2O)_2(4\text{-acetylpyridine})_2$ (M = Co, Ni) will form.[63, 64] For these samples AAS proves, that the Co:Ni ratio of the mixed crystals exactly corresponds to that used in the synthesis (Table S3). XRPD measurement shows that the 043 reflection of this batch is located exactly between that of the physical mixture, indicating for mixed crystal formation (Figure S9). However, the full width at half maximum (FWHM) is much broader than that of the homometallic compounds, indicating that crystals of a variety of compositions were obtained (Figure S9). Scanning electron microscopy (SEM) of these mixed crystals and the homometallic compounds indicates, that the broadening cannot be traced back to large differences in the particle size (Figure S10). The formation of inhomogeneous samples is further confirmed by EDX

measurements of selected crystals, that show significant deviations from the expected Co:Ni ratio (Table S4) and this is also in agreement with magnetic and heat capacity measurements (see below). The formation of inhomogeneous samples might originate from the different solubility and dissolution rate of the metal salts in ethanol and the fact that using small amounts of solvent the metal salts are not completely dissolved. Moreover, the sequence of adding the reactants is also of importance, because if, e.g. $Ni(NCS)_2$ is added first to the mixture with ligand before $Co(NCS)_2$, Ni-rich particles can precipitate in the beginning and would become Co-rich with increasing reaction time. This would also explains that after complete precipitation the ratio between Co and Ni will correspond to that used in the synthesis. For the synthesis of the homometallic compounds it is unimportant and if only a very small amount of solvent is used it is of advantage, because the products are obtained in high yield.

However, concerning the stability of mixed crystals one would assume that they are more stable than the homometallic counterparts because of entropy and thus, one would expect formation of homogenous samples with increasing reaction time. Therefore, we prepared a suspension of equivalent amounts of **1-Co** and **1-Ni** with large excess of solid in ethanol, which was stirred for 30 d. Investigations of the residue by AAS reveal, that mixed crystals with x close to 0.5 are obtained, which according to XRPD measurements should be homogenous (Figure S11). For such a sample the Co and Ni concentration in a saturated solution was measured by AAS using the same procedure as that used to determine the solubility of the individual compounds. These values are lower than that of the homometallic compounds, which also points to a higher stability (Table S5).

Based on the above described results we prepared mixed crystals by adding 4-acetylpyridine to clear solutions of $Co(NCS)_2$ and $Ni(NCS)_2$ in ethanol at room-temperature but also at elevated temperatures. Independent of the reaction time or temperature, always samples were obtained, in which the Co:Ni ratio corresponds exactly to that used in the synthesis, as proven by AAS measurements (Table S6) EDX measurements of selected crystals indicate the formation of homogenous samples (Table S7). This is

further supported by DSC measurements where in contrast to the physical mixtures only one thermal event is observed (Figure S12). Mixed crystal formation is also indicated by XRPD measurements, where two peaks are observed for the 043 reflection in the physical mixtures, whereas only one peak is visible for the mixed crystals (Figure 2 and Figure S13).

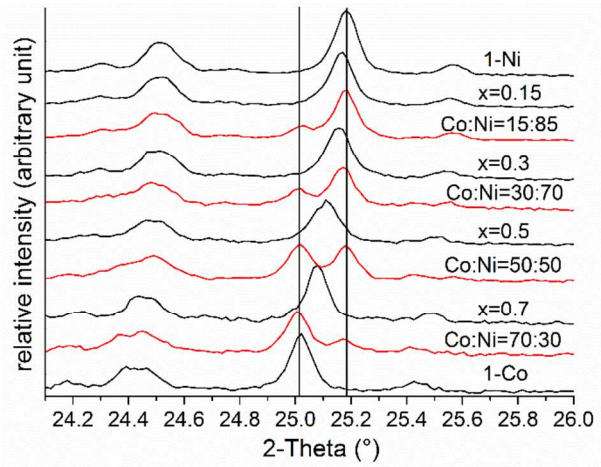

Figure 2. XRPD pattern of **1-Co, 1-Ni** and **1-Co$_x$Ni$_{1-x}$** (x = 0.15, 0.3, 0.5, and 0.7; black) and of physical mixtures of **1-Co** and **1-Ni** with the same Co:Ni ratio (red). For the full range see Figure S13.

It is also visible that, with increasing Ni content, the 043 reflection shifts to higher Bragg angles. If the FWHM of the reflections of the mixed crystals is compared with that of the physical mixture and that of an inhomogenous sample as described above, it is strongly indicated that by this procedure homogenous samples are obtained.

For these mixed crystals the unit cell volume was determined from Pawley fits [65] using XRPD patterns measured at room-temperature, which shows a linear increase with increasing Ni content. This nicely proves that Vegard's law is valid, which is expected for homogenous mixed crystals (Figure 3).[66, 67]

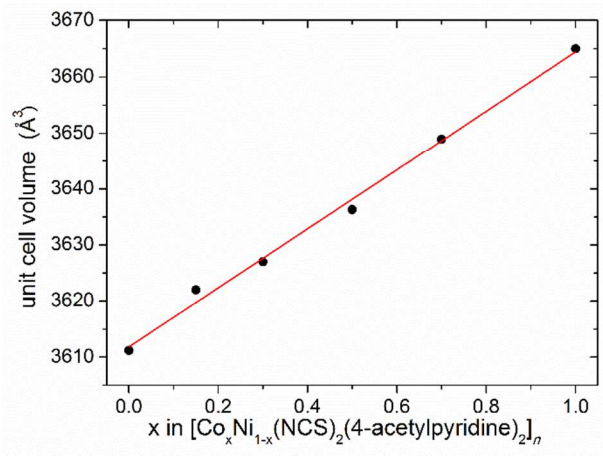

Figure 3. Unit cell volume as function of the Co and Ni content in **1-Co$_x$Ni$_{1-x}$** (x = 0, 0.15, 0.3, 0.5, 0.7 and 1.0).

Magnetic and heat-capacity measurements. To investigate the influence of mixed crystal formation on the magnetic properties, the temperature dependence of the susceptibility χ was measured at 100 Oe for **1-Co$_x$Ni$_{1-x}$** but also for **1-Co** and **1-Ni** (Figure 4). For **1-Ni** the susceptibility increases significantly starting at about 10 K and at about 2 K nearly saturation is observed, which is in agreement with its ferromagnetic behavior, already reported in literature.[61] With decreasing Ni content the temperature at which the susceptibility starts to increase moves to lower temperatures and one can anticipate that saturation might be reached at below 2 K. For **1-Co** the χ vs. T curve looks like that for a paramagnet, which can be traced back to the fact that magnetic ordering occurs at a temperature that is below the lowest temperature available in the used magnetometer (Figure 4). The room-temperature values of χT vary between 1.21 cm^3 K mol^{-1} for the Ni and 3.35 cm^3 K mol^{-1} for the Co compound, which is in the range typically observed for these cations in an octahedral coordination.[61, 68-71] For all compounds the magnetic behavior changes continuously as function of the actual Co:Ni ratio (Figure S14 and S15).

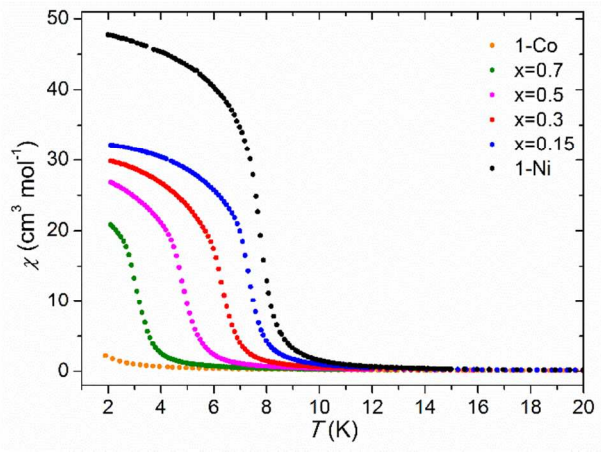

Figure 4. Temperature dependence of the magnetic susceptibility at 100 Oe measured for **1-Co, 1-Ni** and **1-Co_xNi_{1-x}** (x = 0.15, 0.3, 0.5, and 0.7). Only the low temperature range is shown.

The field dependence of the magnetization of **1-Ni** measured at 2.1 K shows a behavior typical for a ferromagnet with nearly saturation at high fields (Figure S16). With increasing Co content the magnetization is modified in the range 0-15 kOe, indicating that significant anisotropy is introduced even by x = 0.15 admixture of Co. The saturation magnetization for the mixed crystals is in between that of the homometallic counterparts and increases with increasing Co content (Figure S16). To get some idea how the critical temperature changes as function of the actual Co:Ni ratio, the first derivative of $\chi(T)$ was plotted as function of temperature, which shows that the critical temperature shifts to lower temperatures with increasing Co content (Figure 5).

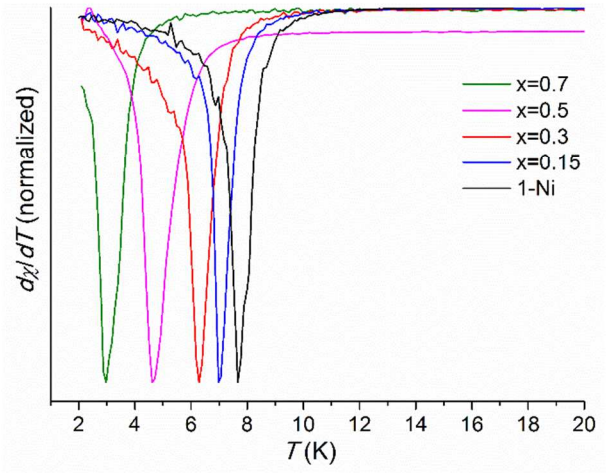

Figure 5. First derivative of the dc susceptibility for **1-Co, 1-Ni** and **1-Co$_x$Ni$_{1-x}$** (x = 0.15, 0.3, 0.5, and 0.7) measured as function of temperature at 100 Oe. Please note that for **1-Co** the critical temperature is at too low temperatures.

To prove the magnetic ordering for the mixed crystals, heat capacity measurements down to 0.4 K were performed, from which the critical temperatures might be determined more precisely. For all samples a lambda-type peak is observed, which points to a second order phase transition (Figure 6).

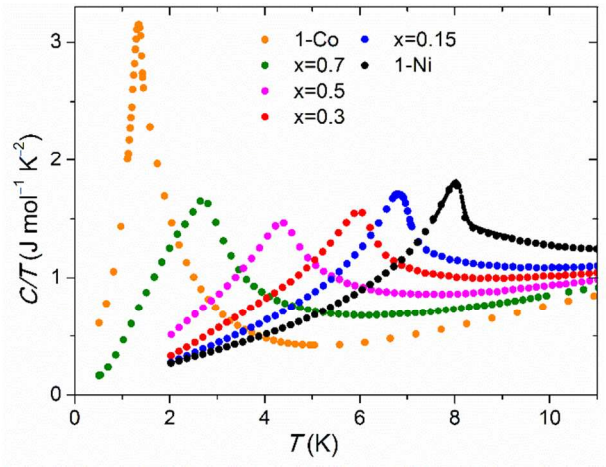

Figure 6. Temperature dependence of the low-temperature specific heat *C* measured for **1-Co, 1-Ni** and **1-Co$_x$Ni$_{1-x}$** (x = 0.15, 0.3, 0.5, and 0.7).

This confirms, that all mixed crystals show a long-range ordering as already observed for **1-Co** and **1-Ni** [61] and excludes a spin-glass behavior. The ac susceptibility shows a maximum of $\chi'(T)$ at temperature that does not depend on the ac frequency, which is also against a spin-glass phase, and in favor of the long range ordering (Figure S18). As the spin-glass ground state would be expected in case of competing FM-AFM exchange interactions in disordered Ni-Co lattice, the presence of the second order transition for all compositions also suggests that all exchange interactions, also between Ni and Co pairs, are ferromagnetic.

From the heat-capacity measurements the values for the critical temperatures were extracted and plotted as function of the actual Co:Ni ratio, which shows that T_c decreases with increasing Co content almost linearly (Figure 6). The values obtained from $d\chi/dT$ are in very good agreement with that obtained from the heat-capacity measurements (Figure 6).

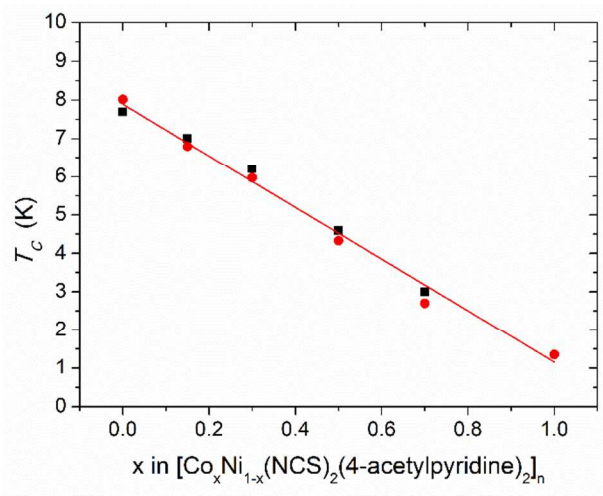

Figure 6. Critical temperature of magnetic ordering for **1-Co$_x$Ni$_{1-x}$** (x = 0, 0.15, 0.3, 0.5, 0.7 and 1.0) as determined from specific heat (red points) and magnetic measurements (black points).

Finally, we also investigated one sample with x = 0.5 by magnetic and heat-capacity measurements for which XRPD measurements indicate inhomogeneity (see above and Figure S11). In this case one would expect broad peaks of $d\chi/dT$, because if each crystal has a different Co:Ni ratio it will exhibits his own transition temperature. This is exactly observed in the magnetic measurements and it is obvious that $d\chi/dT$

starts to decrease at higher temperatures, which clearly proves that Ni-rich particles are present (Figure S19). This is further confirmed by heat-capacity measurements, for which a behavior with at least two distinct broad maxima is observed (Figure S20).

CONCLUSION

In the present contribution we have shown that the critical temperatures of coordination compounds can be tuned by mixed crystal formation. This was proven using layered compounds with the general composition $[M(NCS)_2(4\text{-acetylpyridine})_2]_n$ (M = Co, Ni), that show dominating ferromagnetic interactions within the layers and magnetic ordering at low temperatures. For the mixed crystals the same behavior was observed with the ferromagnetic ordering and no sign for the formation of a spin-glass and it was found that the critical temperature increases linear with increasing Ni content. However, in this case homogenous samples are needed, because otherwise each of the particles exhibits its own transition temperature leading to no definite transition, as proven by magnetic and heat-capacity measurements. This cannot be achieved by simply reacting all reactants in an arbitrary order in a small amount of solvent for a limited time, because depending on the solubility and dissolution behavior of the reactants and the products as well as the order in which the reactants are added, the composition of each particle can be different. However, even from inhomogeneous samples homogenous mixed crystals can form using very long reaction time, which indicates that the mixed crystals seem to be more stable. To prove mixed crystal formation and the homogeneity of samples, different methods should be applied and it this case XRPD represents a powerful tool, even if both compounds are isotypic with cations neighbored in the periodic table and consequently very similar XRPD patterns.

ACKNOWLEDGEMENTS

This project was supported by the Deutsche Forschungsgemeinschaft (Project No. Na 720/6-1) and the State of Schleswig-Holstein and by National Science Centre, Poland (project no. 2017/25/B/ST3/00856). We thank Prof. Dr. Wolfgang Bensch for access to his experimental facilities.

ASSOCIATED CONTENT

The Supporting Information is available free of charge on the ACS Publications website at DOI:

AUTHOR INFORMATION

Corresponding Author

*Email: cnaether@ac.uni-kiel.de.

Notes

The authors declare no competing financial interest.

References

(1) Coulon, C.; Pianet, V.; Urdampilleta, M.; Clérac, R. *Single-Chain Magnets and Related Systems*. Springer Berlin Heidelberg: 2015; Vol. 164, p 143-184.
(2) Zhang, W.-X.; Ishikawa, R.; Breedlovea, B.; Yamashita, M. Single-chain magnets: beyond the Glauber model. *RSC Adv.* **2013,** *3*, 3772-3798.
(3) Wang, X. Y.; Avendano, C.; Dunbar, K. R. Molecular magnetic materials based on 4d and 5d transition metals. *Chem. Soc. Rev.* **2011,** *40*, 3213-3238.
(4) Weng, D.-F.; Wang, Z.-M.; Gao, S. Framework structured weak ferromagnets. *Chem. Soc. Rev.* **2011,** *40*, 3157-3181.
(5) Talham, D. R.; Meisel, M. W. Thin films of coordination polymer magnets. *Chem. Soc. Rev.* **2011,** *40*, 3356-3365.
(6) Dhers, S.; Feltham, H. L. C.; Brooker, S. A toolbox of building blocks, linkers and crystallisation methods used to generate single-chain magnets. *Coord. Chem. Rev.* **2015,** *296*, 24-44.
(7) Dechambenoit, P.; Long, J. R. Microporous magnets. *Chem. Sci. Rev.* **2011,** *40*, 3249-3265.
(8) Miller, J. S. Magnetically ordered molecule-based materials. *Chem. Soc. Rev.* **2011,** *40*, 3266-3296.
(9) Mroziński, J.; Kłak, J.; Kruszyński, R. Crystal structure and magnetic properties of the 1D bimetallic thiocyanate bridged compound: {(CuL1)[Co(NCS)4]}(L1=N-rac-5,12-Me2-[14]-4,11-dieneN4). *Polyhedron* **2008,** *27*, 1401-1407.

(10) Machura, B.; Świtlicka, A.; Zwoliński, P.; Mroziński, J.; Kalińska, B.; Kruszynski, R. Novel bimetallic thiocyanate-bridged Cu(II)–Hg(II) compounds—synthesis, X-Ray studies and magnetic properties. *J. Solid State Chem.* **2013,** *197*, 218-227.
(11) Guo, J.-F.; Wang, X.-T.; Wang, B.-W.; Xu, G.-C.; Gao, S.; Szeto, L.; Wong, W.-T.; Wong, W.-Y.; Lau, T.-C. One-Dimensional Ferromagnetically Coupled Bimetallic Chains Constructed with trans-[Ru(acac)2(CN)2]−: Syntheses, Structures, Magnetic Properties, and Density Functional Theoretical Study. *Chem. – Eur. J.* **2010,** *16*, 3524-3535.
(12) Chorazy, S.; Rams, M.; Hoczek, A.; Czarnecki, B.; Sieklucka, B.; Ohkoshi, S.; Podgajny, R. Structural anisotropy of cyanido-bridged {CoII9WV6} single-molecule magnets induced by bidentate ligands: towards the rational enhancement of an energy barrier. *Chem. Commun.* **2016,** *52*, 4772-4775.
(13) Dul, M.-C.; Pardo, E.; Lescouëzec, R.; Journaux, Y.; Ferrando-Soria, J.; Ruiz-García, R.; Cano, J.; Julve, M.; Lloret, F.; Cangussu, D.; Pereira, C. L. M.; Stumpf, H. O.; Pasán, J.; Ruiz-Pérez, C. Supramolecular coordination chemistry of aromatic polyoxalamide ligands: A metallosupramolecular approach toward functional magnetic materials. *Coordination Chemistry Reviews* **2010,** *254*, 2281-2296.
(14) Martínez-Lillo, J.; Faus, J.; Lloret, F.; Julve, M. Towards multifunctional magnetic systems through molecular-programmed self assembly of Re(IV) metalloligands. *Coord. Chem. Rev.* **2015,** *289-290*, 215-237.
(15) Cowan, M. G.; Brooker, S. Syntheses, structures and properties of structurally characterised complexes of imide-based ligands. *Coord. Chem. Rev.* **2012,** *256*, 2944-2971.
(16) Pedersen, K. S.; Bendix, J.; Clerac, R. Single-molecule magnet engineering: building-block approaches. *Chem. Commun.* **2014,** *50*, 4396-4415.
(17) Li, Y.-H.; He, W.-R.; Ding, X.-H.; Wang, S.; Cui, L.-F.; Huang, W. Cyanide-bridged assemblies constructed from capped tetracyanometalate building blocks [MA(ligand)(CN)4]1−/2− (MA=Fe or Cr). *Coord. Chem. Rev.* **2012,** *256*, 2795-2815.
(18) Wang, S.; Ding, X.-H.; Li, Y.-H.; Huang, W. Dicyanometalate chemistry: A type of versatile building block for the construction of cyanide-bridged molecular architectures. *Coord. Chem. Rev.* **2012,** *256*, 439-464.
(19) Newton Graham, N.; Nihei, M.; Oshio, H. Cyanide-Bridged Molecular Squares – The Building Units of Prussian Blue. *Eur. J. Inorg. Chem.* **2011,** *2011*, 3031-3042.
(20) Wang, S.; Ding, X.-H.; Zuo, J.-L.; You, X.-Z.; Huang, W. Tricyanometalate molecular chemistry: A type of versatile building blocks for the construction of cyano-bridged molecular architectures. *Coord. Chem. Rev.* **2011,** *255*, 1713-1732.
(21) Lescouëzec, R.; Toma, L. M.; Vaissermann, J.; Verdaguer, M.; Delgado, F. S.; Ruiz-Pérez, C.; Lloret, F.; Julve, M. Design of single chain magnets through cyanide-bearing six-coordinate complexes. *Coordination Chemistry Reviews* **2005,** *249*, 2691-2729.
(22) Sieklucka, B.; Podgajny, R.; Przychodzeń, P.; Korzeniak, T. Engineering of octacyanometalate-based coordination networks towards functionality. *Coord. Chem. Rev* **2005,** *249*, 2203-2221.
(23) Nowicka, B.; Reczynski, M.; Rams, M.; Nitek, W.; Koziel, M.; Sieklucka, B. Larger pores and higher Tc: {[Ni(cyclam)]3[W(CN)8]2[middle dot]solv}n - a new member of the largest family of pseudo-polymorphic isomers among octacyanometallate-based assemblies. *CrystEngComm* **2015,** *17*, 3526-3532.
(24) Ru, J.; Gao, F.; Wu, T.; Yao, M.-X.; Li, Y.-Z.; Zuo, J.-L. Enantiopure heterobimetallic single-chain magnets from the chiral RuIII building block. *Dalton Trans.* **2014,** *43*, 933-936.
(25) Chorazy, S.; Stanek, J. J.; Nogas, W.; Majcher, A. M.; Rams, M.; Koziel, M.; Juszynska-Galazka, E.; Nakabayashi, K.; Ohkoshi, S.; Sieklucka, B.; Podgajny, R. Tuning of Charge Transfer Assisted Phase Transition and Slow Magnetic Relaxation Functionalities in $\{Fe_{9-x}Co_x[W(CN)_8]_6\}$ (x = 0-9) Molecular Solid Solution. *J. Am. Chem. Soc.* **2016,** *138*, 1635-46.

(26) Wang, Y. Q.; Yue, Q.; Gao, E. Q. Effects of Metal Blending in Random Bimetallic Single-Chain Magnets: Synergetic, Antagonistic, or Innocent. *Chem. Eur. J.* **2017,** *23*, 896-904.
(27) Erickson, P. K.; Miller, J. S. Thin film Co[TCNE]2 and VyCo1−y[TCNE]2 magnetic materials. *J. Magn. Magn. Mat.* **2012,** *324*, 2218-2223.
(28) Vickers, E. B.; Senesi, A.; Miller, J. S. Ni[TCNE]2·zCH2Cl2 (Tc=13 K) and VxNi1−x[TCNE]y·zCH2Cl2 solid solution room temperature magnets. *Inorg. Chim. Acta* **2004,** *357*, 3889-3894.
(29) Pokhodnya, K. I.; Vickers, E. B.; Bonner, M.; Epstein, A. J.; Miller, J. S. Solid Solution VxFe1-x[TCNE]2·zCH2Cl2 Room-Temperature Magnets. *Chem. Mater.* **2004,** *16*, 3218-3223.
(30) Sugimoto, M. The Past, Present, and Future of Ferrites. *J. Am. Ceram. Soc* **1999,** *82*, 269-280.
(31) Adachi, S. GaAs, AlAs, and AlxGa1−xAs: Material parameters for use in research and device applications. *J. Appl. Phys.* **1985,** *58*, R1-R29.
(32) Bednorz, J. G.; Müller, K. A. Possible highTc superconductivity in the Ba−La−Cu−O system. *Z. Phys. B* **1986,** *64*, 189-193.
(33) Ramirez, A. P. Colossal magnetoresistance. *J. Phys.: Condens. Matter* **1997,** *9*, 8171.
(34) Wöhlert, S.; Fic, T.; Tomkowicz, Z.; Ebbinghaus, S. G.; Rams, M.; Haase, W.; Näther, C. Structural and Magnetic Studies of a New Co(II) Thiocyanato Coordination Polymer Showing Slow Magnetic Relaxations and a Metamagnetic Transition. *Inorg. Chem.* **2013,** *52*, 12947-12957.
(35) Rams, M.; Tomkowicz, Z.; Böhme, M.; Plass, W.; Suckert, S.; Werner, J.; Jess, I.; Näther, C. Influence of the Metal Coordination and the Co-ligand on the Relaxation Properties of 1D $Co(NCS)_2$ Coordination Polymers. *Phys. Chem. Chem. Phys.* **2017,** *19*, 3232-3243.
(36) Wöhlert, S.; Wriedt, M.; Fic, T.; Tomkowicz, Z.; Haase, W.; Näther, C. Synthesis, Crystal Structure and Magnetic Properties of the Coordination Polymer $[Fe(NCS)_2(1,2\text{-bis}(4\text{-pyridyl})\text{-ethylene})]_n$ Showing a Two Step Metamagnetic Transition *Inorg. Chem.* **2013,** *52*, 1061-1068.
(37) Wöhlert, S.; Tomkowicz, Z.; Rams, M.; Ebbinghaus, S. G.; Fink, L.; Schmidt, M. U.; Näther, C. Influence of the Co-Ligand on the Magnetic and Relaxation Properties of Layered Co(II) Thiocyanato Coordination Polymers. *Inorg. Chem.* **2014,** *53*, 8298–8310.
(38) Wöhlert, S.; Runčevski, T.; Dinnebier, R. E.; Ebbinghaus, S. G.; Näther, C. Synthesis, Structures, Polymorphism, and Magnetic Properties of Transition Metal Thiocyanato Coordination Compounds. *Cryst. Growth Des.* **2014,** *14*, 1902-1913.
(39) Wöhlert, S.; Ruschewitz, U.; Näther, C. Metamagnetism and Slow Relaxation of the Magnetization in the 2D Coordination Polymer: [Co(NCSe)2(1,2-bis(4-pyridyl)ethylene)]n. *Cryst. Growth Des.* **2012,** *12*, 2715-2718.
(40) Prananto, Y. P.; Urbatsch, A.; Moubaraki, B.; Murray, K. S.; Turner, D. R.; Deacon, G. B.; Batten Stuart, R. Transition Metal Thiocyanate Complexes of Picolylcyanoacetamides. *Aust. J. Chem.* **2017,** *70*, 516-528.
(41) Neumann, T.; Ceglarska, M.; Rams, M.; Germann, L. S.; Dinnebier, R. E.; Suckert, S.; Näther, C. Structures, thermodynamic relations and magnetism of novel stable and metastable $Ni(NCS)_2$ coordination polymers. *Inorg. Chem.* **2018,** *57*, 3305-3314.
(42) González, R.; Acosta, A.; Chiozzone, R.; Kremer, C.; Armentano, D.; De Munno, G.; Julve, M.; Lloret, F.; Faus, J. New Family of Thiocyanate-Bridged Re(IV)-SCN-M(II) (M = Ni, Co, Fe, and Mn) Heterobimetallic Compounds: Synthesis, Crystal Structure, and Magnetic Properties. *Inorg. Chem.* **2012,** *51*, 5737-5747.
(43) Palion-Gazda, J.; Machura, B.; Lloret, F.; Julve, M. Ferromagnetic Coupling Through the End-to-End Thiocyanate Bridge in Cobalt(II) and Nickel(II) Chains. *Cryst. Growth Des.* **2015,** *15*, 2380-2388.

(44) Massoud, S. S.; Guilbeau, A. E.; Luong, H. T.; Vicente, R.; Albering, J. H.; Fischer, R. C.; Mautner, F. A. Mononuclear, dinuclear and polymeric 1D thiocyanato- and dicyanamido–copper(II) complexes based on tridentate coligands. *Polyhedron* **2013,** *54*, 26-33.
(45) Guillet, J. L.; Bhowmick, I.; Shores, M. P.; Daley, C. J. A.; Gembicky, M.; Golen, J. A.; Rheingold, A. L.; Doerrer, L. H. Thiocyanate-Ligated Heterobimetallic {PtM} Lantern Complexes Including a Ferromagnetically Coupled 1D Coordination Polymer. *Inorg. Chem.* **2016,** *55*, 8099-8109.
(46) Shurdha, E.; Lapidus, S. H.; Stephens, P. W.; Moore, C. E.; Rheingold, A. L.; Miller, J. S. Extended Network Thiocyanate- and Tetracyanoethanide-Based First-Row Transition Metal Complexes. *Inorg. Chem.* **2012,** *51*, 9655-9665.
(47) Shurdha, E.; Moore, C. E.; Rheingold, A. L.; Lapidus, S. H.; Stephens, P. W.; Arif, A. M.; Miller, J. S. First Row Transition Metal(II) Thiocyanate Complexes, and Formation of 1-, 2-, and 3-Dimensional Extended Network Structures of M(NCS)2(Solvent)2 (M = Cr, Mn, Co) Composition. *Inorg. Chem.* **2013,** *52*, 10583-10594.
(48) Kabesová, M.; Boca, R.; Melník, M.; Valigura, D.; Dunaj-Jurco, M. Bonding properties of thiocyanate groups in copper(II) and copper(I) complexes. *Coord. Chem. Rev* **1995,** *140*, 115-135.
(49) Buckingham, D. A. The linkage isomerism of thiocyanate bonded to cobalt (III). *Coord. Chem. Rev.* **1994,** *135*, 587-621.
(50) Petrosyants, S.; Dobrokhotova, Z.; Ilyukhin, A.; Efimov, N.; Mikhlina, Y.; Novotortsev, V. Europium and terbium thiocyanates: Syntheses, crystal structures, luminescence and magnetic properties. *Inorg. Chim. Acta* **2015,** *434*, 41-50.
(51) Uhrecký, R.; Ondrejkovičová, I.; Lacková, D.; Fáberová, Z.; Mroziński, J.; Kalińska, B.; Padělková, Z.; Koman, M. New thiocyanato iron(II) complex with 3,5-bis(3-pyridyl)-1,2,4-thiadiazole: Synthesis, structure, magnetic and spectral properties. *Inorg. Chim. Acta* **2014,** *414*, 33-38.
(52) Adams, C. J.; Haddow, M. F.; Harding, D. J.; Podesta, T. J.; Waddington, R. E. Iron(ii) thio- and selenocyanate coordination networks containing 3,3[prime or minute]-bipyridine. *CrystEngComm* **2011,** *13*, 4909-4914.
(53) Palion-Gazda, J.; Gryca, I.; Maroń, A.; Machura, B.; Kruszynski, R. Thiocyanate cadmium(II) coordination compounds with 2,3,5,6-tetrakis(2-pyridyl)pyrazine – Synthesis, structure and luminescent properties. *Polyhedron* **2017,** *135*, 109-120.
(54) Mautner, F. A.; Fischer, R. C.; Rashmawi, L. G.; Louka, F. R.; Massoud, S. S. Structural characterization of metal(II) thiocyanato complexes derived from bis(2-(H-pyrazol-1-yl)ethyl)amine. *Polyhedron* **2017,** *124*, 237-242.
(55) Petrosyants, S. P.; Dobrokhotova, Z. V.; Ilyukhin, A. B.; Efimov, N. N.; Gavrikov, A. V.; Vasilyev, P. N.; Novotortsev, V. M. Mononuclear Dysprosium Thiocyanate Complexes with 2,2′-Bipyridine and 1,10-Phenanthroline: Synthesis, Crystal Structures, SIM Behavior, and Solid-Phase Transformations. *Eur. J. Inorg. Chem.* **2017,** *2017*, 3561-3569.
(56) Mekuimemba, C. D.; Conan, F.; Mota, A. J.; Palacios, M. A.; Colacio, E.; Triki, S. On the Magnetic Coupling and Spin Crossover Behavior in Complexes Containing the Head-to-Tail [FeII2(μ-SCN)2] Bridging Unit: A Magnetostructural Experimental and Theoretical Study. *Inorg. Chem.* **2018,** *57*, 2184-2192.
(57) Rams, M.; Böhme, M.; Kataev, V.; Krupskaya, Y.; Büchner, B.; Plass, W.; Neumann, T.; Tomkowicz, Z.; Näther, C. Static and dynamic magnetic properties of the ferromagnetic coordination polymer $[Co(NCS)_2(py)_2]_n$. *Phys. Chem. Chem. Phys.* **2017,** *19*, 24534-24544.
(58) Suckert, S.; Rams, M.; Rams, M. M.; Näther, C. Reversible and topotactic solvent removal in a magnetic $Ni(NCS)_2$ coordination polymer. *Inorg. Chem.* **2017,** *56*, 8007–8017.

(59) Werner, J.; Tomkowicz, Z.; Reinert, T.; Näther, C. Synthesis, Structure, and Properties of Coordination Polymers with Layered Transition-Metal Thiocyanato Networks. *Eur. J. Inorg. Chem.* **2015,** 3066-3075.
(60) Suckert, S.; Rams, M.; Germann, L.; Cegiełka, D. M.; Dinnebier, R. E.; Näther, C. Thermal transformation of a 0D thiocyanate precursor into a ferromagnetic 3D coordination network via a layered intermediate. *Cryst. Growth Des.* **2017,** *17*, 3997–4005.
(61) Suckert, S.; Rams, M.; Böhme, M.; Germann, L. S.; Dinnebier, R. E.; Plass, W.; Werner, J.; Näther, C. Synthesis, structures, magnetic and theoretical investigations of Co and Ni coordination polymers with layered thiocyanate networks. *Dalton Trans.* **2016,** *45*, 18190-18201.
(62) Werner, J.; Runčevski, T.; Dinnebier, R.; Ebbinghaus, S. G.; Suckert, S.; Näther, C. Thiocyanato Coordination Polymers with Isomeric Coordination Networks – Synthesis, Structures, and Magnetic Properties. *Eur. J. Inorg. Chem.* **2015,** 3236-3245.
(63) Werner, J.; Rams, M.; Tomkowicz, Z.; Runčevski, T.; Dinnebier, R. E.; Suckert, S.; Näther, C. Thermodynamically Metastable Thiocyanato Coordination Polymer that shows Slow Relaxations of the Magnetization. *Inorg. Chem.* **2015,** *54*, 2893-2901.
(64) Drew, M. G. B.; Gray, N. I.; Cabral, M. F.; Cabral, J. d. O. Structures of tetrakis(4-benzoylpyridine)bis(isothiocyanato)cobalt(II) (1) and bis(4-acetylpyridine)diaquabis(isothiocyanato)cobalt(II) (2). *Acta Crystallogr. C* **1985,** *41*, 1434-1437.
(65) Bruker, A. X. S. *TOPAS*, 5.0; 2014.
(66) Denton, A. R.; Ashcroft, N. W. Vegard's law. *Phys. Rev. A* **1991,** *43*, 3161-3164.
(67) Vegard, L. Die Konstitution der Mischkristalle und die Raumfüllung der Atome. *Z. Phys.* **1921,** *5*, 17-26.
(68) Lloret, F.; Julve, M.; Cano, J.; Ruiz-García, R.; Pardo, E. Magnetic properties of six-coordinated high-spin cobalt(II) complexes: Theoretical background and its application. *Inorg. Chim. Acta* **2008,** *361*, 3432-3445.
(69) Nowicka, B.; Reczynski, M.; Rams, M.; Nitek, W.; Zukrowski, J.; Kapusta, C.; Sieklucka, B. Hydration-switchable charge transfer in the first bimetallic assembly based on the $[Ni(cyclam)]^{3+}$ - magnetic CN-bridged chain $\{(H_3O)[Ni^{III}(cyclam)][Fe^{II}(CN)_6]\cdot 5H_2O\}_n$. *Chem. Commun.* **2015,** *51*, 11485-11488.
(70) Tomkowicz, Z.; Ostrovsky, S.; Müller-Bunz, H.; Eltmimi, A. J. H.; Rams, M.; Brown, D. A.; Haase, W. Extended Triple-Bridged Ni(II)- and Co(II)-Hydroxamate Trinuclear Complexes: Synthesis, Crystal Structures, and Magnetic Properties. *Inorg. Chem.* **2008,** *47*, 6956-6963.
(71) Manson, J. L.; Kmety, C. R.; Huang, Q.-z.; Lynn, J. W.; Bendele, G. M.; Pagola, S.; Stephens, P. W.; Liable-Sands, L. M.; Rheingold, A. L.; Epstein, A. J.; Miller, J. S. Structure and Magnetic Ordering of MII[N(CN)2]2 (M = Co, Ni). *Chem. Mater.* **1998,** *10*, 2552-2560.

Received: ((will be filled in by the editorial staff))

Published online: ((will be filled in by the editorial staff))

Entry for the Table of Contents

Tuning of the critical temperature in magnetic 2D coordination polymers by mixed crystal formation

Carsten Wellm, Michał Rams, Tristan Neumann, Magdalena Ceglarska, and Christian Näther

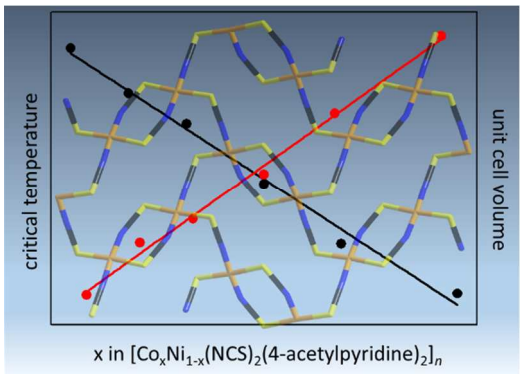

Mixed crystals of a layered coordination polymer with the composition [$Co_xNi_{1-x}(NCS)_2$(4-acetylpyridine)$_2$]$_n$ were prepared and characterized by XRPD, EDX, AAS, DSC, magnetic and heat capacity measurements, which show that the critical temperature of magnetic ordering depends linearly on the actual Co and Ni content.

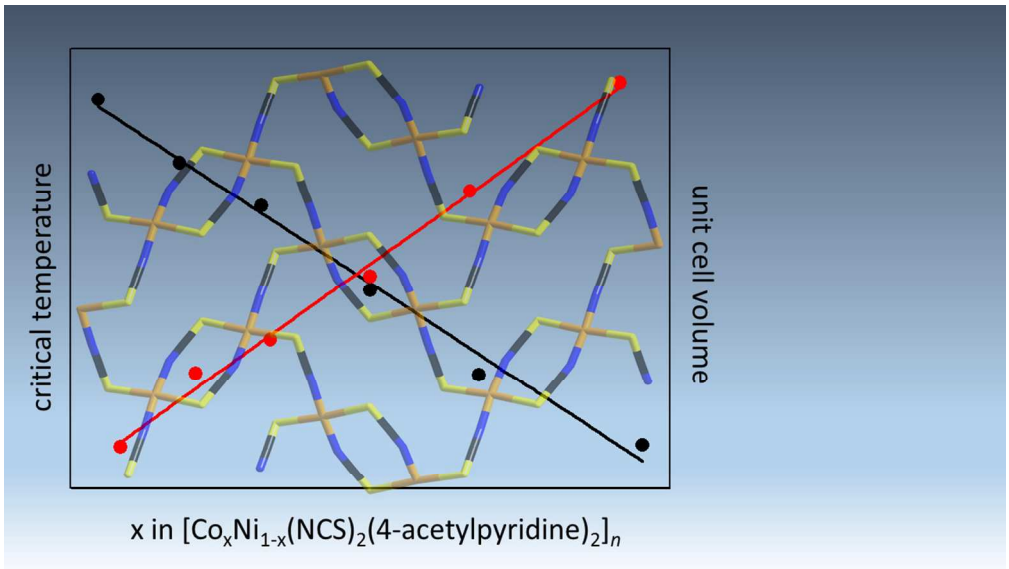

Figure for the table of contents

338x190mm (96 x 96 DPI)